Adhesion Interactions between Poly(vinyl alcohol) and Iron-Oxide Surfaces: The Effect of Acetylation

B. Uner,[1] M. K. Ramasubramanian,[2] S. Zauscher,[3] J. F. Kadla[1,4]

[1]*Department of Wood and Paper Science, North Carolina State University, Raleigh, North Carolina 27695*
[2]*Mechanical and Aerospace Engineering Department, North Carolina State University, Raleigh, North Carolina 27695*
[3]*Department of Mechanical Engineering and Materials Science, Duke University, Durham, North Carolina 27708*
[4]*Department of Wood Science, University of British Columbia, Vancouver, British Columbia V6T 1Z4, Canada*

Received 9 November2004; accepted 27 April 2005
DOI 10.1002/app.22980
Published online 19 January 2006 in Wiley InterScience (www.interscience.wiley.com).

ABSTRACT: Atomic force microscopy with chemically functionalized colloidal probes was used to study "acid–base" interactions between poly(vinyl alcohol) (PVA) and a metal surface. By using well-defined model surfaces, we have studied the adhesion forces between a hydroxylated surface and cantilever tips with varying hydroxyl content. Decreasing the amount of available hydroxyl groups dramatically reduced the observed adhesion force. The calculated bond energy for each cantilever tip was found to be in the range of typical hydrogen bond energies, i.e., 10–40 kJ/mol, suggesting that the acid–base interactions are predominately hydrogen bonding. Similarly, the force versus distance curves using PVA functionalized colloidal probes showed a strong dependence on the chemical functionality of the tip and the degree of acetylation of the intervening PVA. It was observed that, with an increase in the acetyl content of the PVA, the adhesion force decreased. © 2006 Wiley Periodicals, Inc. J Appl Polym Sci 99: 3528–3534, 2006

Key words: adhesion; atomic force microscopy (AFM); FTIR; poly(vinyl alcohol)

INTRODUCTION

When surfaces come in intimate molecular contact, adhesion arises from a number of intermolecular forces, including van der Waals interactions, hydrogen bonding, and attractive electrostatic forces.[1–3] Although many tests, usually carried out on a mechanical testing machine, have been developed to measure adhesive bond strength,[4] they are unable to detect adhesion on the molecular level. However, it is the molecular level understanding of the adhesion phenomena that is required to better understand and control adhesion in often complex industrial situations. The adhesion of polymers to surfaces is fundamentally important in many industrial processes and applications. The creping process used in tissue paper manufacturing is a good example. An understanding of the adhesion mechanism between these surfaces is important in paper creping operations used in the manufacture of a variety of low-density paper materials, such as tissue paper.[5,6] Creping is used to develop bulk, stretch, absorbency, and softness in tissue paper.[5] In the creping process, the moist paper web is attached to the cast iron dryer surface with an adhesive, and after drying, scraped from the dryer surface by a doctor blade.[7] Controlling adhesion between the paper web and the drum surface is critical to successful creping. Various techniques have been developed to control the adhesion between the paper web and the metal surface. One method utilizes two adhesives in which the first adhesive is applied directly to the dryer surface and the second adhesive is applied to the paper web. Poly(vinyl alcohol) (PVA) and poly(amidoamine) adhesives are commonly used, because they provide strong adhesion between the paper web and the cast iron surface. It is believed that acid–base interactions are responsible for their adhesive interactions.[8,9] Among other things, controlling the ratio between these two adhesives controls the adhesion and release of the paper from the dryer surface. However, determining the optimal ratio of these adhesives can be difficult owing to variations in drying, as adhesive layers build up on the dryer surface. Another commonly used method to control adhesion is through the addition of debonders, such as quaternary ammonium salts or hydrocarbons, to the adhesive system.[7,9–11] Although these multicomponent systems enable better control of adhesion, they are also complex to handle, which results in high operating costs and requires careful control over the operating conditions. A potentially simpler and more cost-effective way to control

Correspondence to: J. F. Kadla (john.kadla@ubc.ca).

adhesion in creping is through manipulation of acid–base interactions, by changing the chemical functionality of the adhesive. We propose that, by decreasing the number of hydroxyl groups available to interact with the paper web and the iron-oxide surface, the adhesive strength should decrease. This can be accomplished simply by changing the ratio of acetyl to hydroxyl groups in PVA. This paper addresses the effect of acetylation on the adhesion between PVAs and iron-oxide surfaces.

Direct study of the adhesion mechanism at an industrial scale creping system is impractical. To study adhesion mechanism related to the creping process, it is necessary to use model systems that mimic the chemical functionality of the surfaces and allow for the direct measurement of interaction forces. Through chemical force spectroscopy[12,13] and infrared (FTIR) spectroscopy measurements, we demonstrate, in this article, that decreasing amounts of hydroxyl groups in the adhesive decrease adhesion between a silica-glass sphere (cellulose mimic) and an iron-oxide surface (creping drum surface mimic). This decrease in adhesion is likely due to the change in the acid–base interactions of the adhesive with the surfaces, by effectively decreasing the proton-donating capability of the adhesive. Force spectroscopy, using an atomic force microscope,[14] has enabled the study of such interactions at the molecular level.[15–21] These measurements can be further refined by using chemically functionalized cantilever probes[13] or colloidal probes.[18,22,23] To assess the effect of hydroxyl content on adhesion, we measured the pull-off forces between hydroxylated model surfaces and between hydroxylated cantilever tips and an iron-oxide surface. To determine the effect of hydroxyl content on adhesion in the presence of adhesion polymers, we measured the pull-off forces between iron-oxide surfaces and colloidal probes, decorated with PVA of varying degree of acetylation.

EXPERIMENTAL

Materials

All chemicals were used as-received without further purification. Filtered (0.02-μm filter) water (Milli-Q, resistivity 18.2 MΩ cm; Millipore, Bedford, MA) was used for all aqueous solutions. Isopropyl alcohol and heptane (ACS grade) were obtained from Fisher Chemical Company (Fairlawn, NJ). Undecanethiol (95%), 11-mercaptoundecanol (95%), DMSO-d6, and acetone-d6 were obtained from Aldrich Chemical Co. (St. Louis, MO). Dimethyl sulfoxide (DMSO) (ACS grade), pyridine, and acetic anhydride (certified ACS grade) were obtained from Fisher Chemical Co. The cast iron plate was obtained from McMaster-Carr Co. (Atlanta, GA). PVA was obtained from Eastman-Kodak Chemical Co. (Kingsport, TN) with a molecular weight of 93,400 and was 99–100% hydrolyzed.

TABLE I
The Degree of Substitution and Molecular Weights of the PVA/PVAc samples

Polymer sample	Degree of acetylation (%)	Molecular weight (Da)
PVA	0	93,000
PVAc25	25	116,000
PVAc42	42	125,000
PVAc85	85	169,000
PVAc100	100	183,000

PVA acetylation and characterization

PVAc samples were prepared by reacting 200 mg of PVA (93,400 Da, >99% hydrolyzed) with 10 mL of a pyridine/acetic anhydride (2:1 v/v) solution for 10 (PVAc25), 20 (PVAc42), 25 (PVAc85), and 60 (PVAc100) min at 70°C, with continuous stirring. At the end of the reaction, the solution was poured over crushed ice and filtered. The resulting precipitate was then washed with cold water/HCl and dried under vacuum.

^{1}H-NMR (DMSO) δ (ppm) 1.4 (d 2H), 1.7 (s 2H), 2.0 (s 3H), 3.8 (s 1H), 4.5 (t 1H), 5 (s 1H).

The degree of acetylation was calculated from integration of the acetyl group methyl protons, relative to the total spectral integration. The degree of substitution and molecular weights of the respective PVA/PVAc samples are listed in Table I. The PVA solutions were prepared by dispersing the polymer in water and raising the temperature to 85°C with continuous stirring for 1 h to facilitate dissolution; PVAc was dissolved in acetone at room temperature under constant stirring for 1 h.

Surface preparation

Hydroxylated model surfaces were prepared from gold-coated and chemically functionalized glass cover slides. The slides were first coated with an adhesive layer of chromium (Cr) (thickness of 2 nm) followed by a layer of gold (Au) (500 nm thickness) by thermal evaporation. Thiols were dissolved in degassed ethanol to obtain 1 mmol/L impregnation solutions. Self-assembled monolayers of 11-mercaptoundecanol (OH-functionality) were prepared by immersion of the freshly gold-coated substrates in 3 m*M* ethanolic solutions of thiol for at least 12 h.

Model iron-oxide surfaces, mimicking the dryer surface, were prepared from thin 10×10 mm^2 cast iron plates. The plate surface was polished with silicon carbide papers having a grit size ranging from 240 to 4000. Each metal plate was then polished with micropolish alumina powder 1C (Buehler Alpha, Union Carbide, Houston, TX) to have a mirror-like finish.

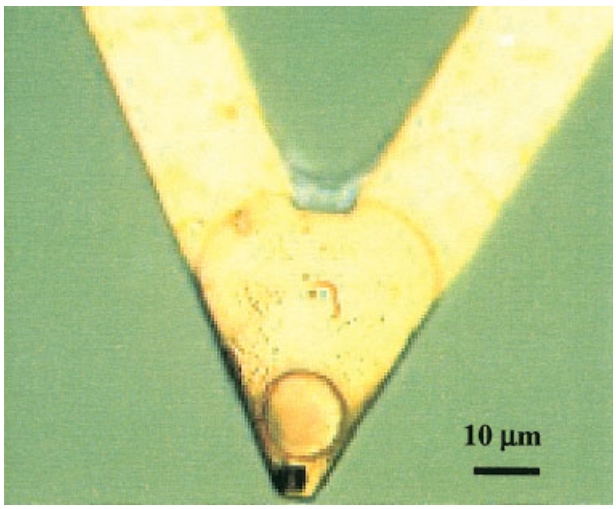

Figure 1 Colloidal probe-modified AFM cantilever. The probe is coated with PVAc42. [Color figure can be viewed in the online issue, which is available at www.interscience.wiley.com.]

Finished surfaces were exhaustively rinsed in ethanol and deionized water and subsequently dried.

Cantilever modification

To prepare cantilevers with varying degree of hydroxylation, gold-coated AFM cantilevers were functionalized[24] by impregnation with mixtures of 11-mercaptoundecanol and dodecanethiol. Thiols were dissolved in degassed ethanol to obtain 3 mmol/L impregnation solutions. Gold coating of the cantilevers was performed in a customized thermal evaporator. First, 15 Å of chromium was deposited as an adhesion promoter, followed by deposition of 200 Å of polycrystalline gold. After gold deposition, the cantilevers were immediately exposed to impregnation solutions for at least 12 h to allow thiol chemisorption. Prior to measurement, the cantilevers were rinsed thoroughly with ethanol and dried under a stream of dry nitrogen gas. Between measurements, the cantilevers were stored in their impregnation solutions. The radius of an AFM tip was deduced from the topographic profiles of step features on gold surfaces obtained from AFM images.[25] Tip radii ranged from 55 to about 117 nm.

Chemically functionalized colloidal probes were prepared by attaching a spherical glass bead (Polysciences Inc., Warrington, PA) to a standard 100-μm long wide-legged triangular, Si_3N_4 cantilever (Model NP), using a one-component, solvent-free, epoxy adhesive (NOA 81; Norland Products, New Brunswick, NJ) (Fig. 1).[18] The epoxy adhesive was crosslinked with UV light (λ = 320 nm) overnight. The glass beads were then coated with PVA or its acetate derivatives by carefully dipping the colloidal probe into a 0.01 g/mL polymer solution. After polymer coating, the probes were dried at 60°C for 1 h.

Cantilever calibration

To assure a linear response of the position sensitive detector (PSD) in adhesion measurements, stiff cantilevers (normal stiffness ~ 0.4 N/m) were used. Normal stiffness was determined from the thermal vibrations of a cantilever suspended in air, by measuring the area of the first resonance peak in a power spectrum.[26] Normal forces were calculated using the PSD sensitivity in the constant compliance regime.

Force spectroscopy

In force spectroscopy, the cantilever spring of the AFM acts as a sensor for the interaction between the cantilever tip and the substrate. The degree of cantilever deflection is a measure of force which can be quantified, in the limit of small deflections, by multiplying with the cantilever spring constant. The force resolution is ultimately limited by the thermal fluctuations of the lever and is typically on the order of piconewtons. Figure 2 shows a typical force displacement curve and schematically corresponding cantilever–substrate interactions. Initially (position A), the cantilever tip and the substrate are far apart, and the cantilever does not experience any force. Once the gradient in the attractive force exceeds the cantilever spring constant, the lever snaps into close, repulsive contact with the substrate surface (B). In the constant

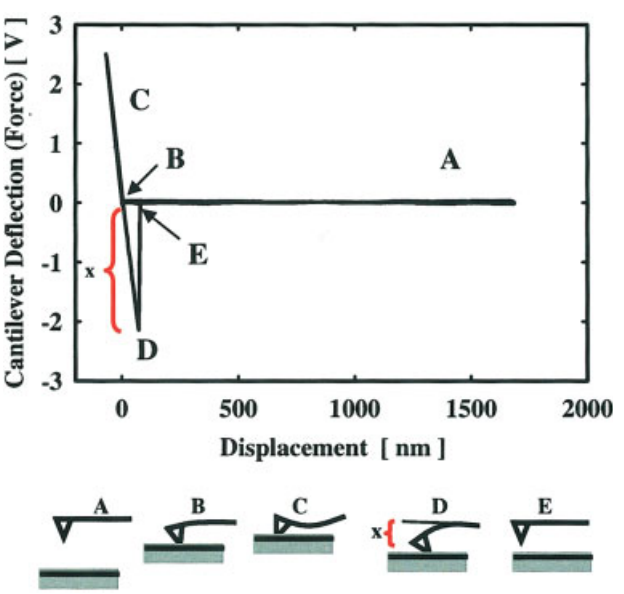

Figure 2 Typical force–displacement curve and schematic representation of the corresponding cantilever–substrate interactions. [Color figure can be viewed in the online issue, which is available at www.interscience.wiley.com.]

compliance regime (C), cantilever and substrate are in contact, and their relative distance is constant. The repulsive force decreases continuously upon retraction until the cantilever snaps out of contact at (D). At this point, the maximal attractive force (adhesion) can be measured. Finally, the cantilever returns into the noncontact regime (E).

A MultiMode™ AFM, equipped with a Nanoscope IIIa controller (Digital Instruments, Santa Barbara, CA), was used to record force extension data (force curves). Measurements were carried out in water using a fluid cell attachment. The adhesion force between functionalized probes and a cast iron surface was determined from the maximum cantilever deflection upon surface retraction, at typical retraction rates of 1 μm/s. The cantilever deflection was converted into an adhesion (pull-off) force by multiplication with the cantilever spring constant, typically 0.45 N/m, determined from the power spectral density of the thermal noise fluctuations (discussed earlier).

Fourier transform infrared spectroscopy

FTIR spectroscopy measurements were made with a Nicolet microscope IR (model Continuum). Polymer solutions were cast on Teflon plates, cleaned, and leveled on a hot plate. One milliliter of a polymer solution was applied to the center of each plate and allowed to spread and dried at 82°C overnight. FTIR measurements were then taken on the film at a resolution of 4 cm^{-1}, using 32 scans, and an area of 50 $\times$ 50 μm^2.

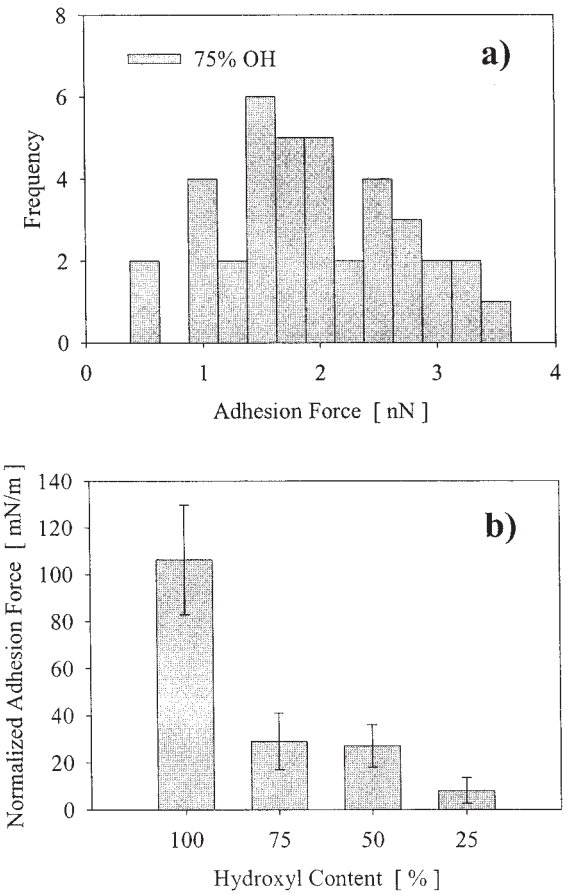

Figure 3 Average adhesion force (normalized by tip radius) between a hydroxylated model surface and cantilever tips modified with different levels of hydroxy-functionalized alkanethiols.

RESULTS AND DISCUSSION

Interaction between hydroxylated model surface and chemically functionalized cantilever tip

To test the hypothesis that adhesion between a metal-oxide surface and a hydroxylated cantilever tip is dependent on the amount of the available hydroxyl groups, we first studied the adhesion of a model system involving a hydroxylated surface and cantilever tips with varying hydroxyl contents. Figure 3(a) shows a typical histogram of adhesion force distribution for the 75% hydroxylated SAM tip interacting with the 100% hydroxylated model surface. Figure 3(b) shows the mean adhesion force (normalized by tip radius) as a function of cantilever tip hydroxyl content. Decreasing the hydroxyl content on the cantilever tip by 25% decreases the adhesion force significantly. Further reduction in hydroxyl content produces much smaller changes in the adhesion force. We would have expected a more linear decrease in the adhesion force with decreasing hydroxyl content; however, the exact hydroxyl content on the tip is unknown. The values reported here reflect the molar ratios of the two thiols used to modify the tip chemistry and it is possible that during self-assembly the thiols partitioned, leading to preferential chemisorption to the gold surface.[27] Nonetheless, adhesion forces decrease with decreasing hydroxyl content of the cantilever tip, which is consistent with a decreasing number of hydroxyl groups able to interact through acid–base interactions with the hydroxylated surface.

It has been proposed that the total adhesion forces between the tip and the sample is the sum of discrete bond forces.[15] The total bond force has a mean value (μ) where $\mu = mF$ and variance (σ^2) where $\sigma^2 = mF^2$ (F = individual bond strength and m = number of bonds). Thus, the ratio of the variance (σ^2) and mean of the total force (μ) gives the individual bond strength ($F = \sigma^2/\mu$). Using this equation, we have calculated the individual bond strength for each cantilever tip and listed the results in Table II.

The hydrogen bond energy may then be calculated using the individual bond strength. To calculate bond energy, eq. (1) was introduced.[10]

TABLE II
Individual Bond Strengths and Bond Energy Measured with Various SAM-Functionalized Tips on a Hydroxylated Model and Iron-Oxide Surface

Functional groups	Mean (nN)	Variance (nN^2)	Individual bond strength (nN)	Bond energy (kJ/mol)
Hydroxylated model surface				
100% OH	12.4	7.55	0.61	32.1
75% OH	1.8	0.57	0.31	16.7
50% OH	2.8	0.88	0.31	16.4
25% OH	0.44	0.08	0.18	10.6
Iron-oxide surface				
100% OH	5.7	4.9	0.88	46.1
75% OH	3.3	1.34	0.40	21.2
50% OH	3.2	2.2	0.71	37.6
25% OH	1.6	0.34	0.22	11.5

$$E = \int_{r_0}^{\infty} -NF(r_0/r)^3\,dr \qquad (1)$$

In this equation, N represents Avogadro's number, F the individual bond strength, and r_0 the hydrogen bond length in water (1.76 Å), respectively. The calculated bond energy for each cantilever tip is included in Table II. These values are in the range of typical hydrogen bond energies, i.e., 10–40 kJ/mol, [3] suggesting that the acid–base interactions are predominately hydrogen bonding.

Interaction between iron-oxide surface and chemically functionalized cantilever tip

In the next step, we measured the adhesion between our model hydroxylated cantilever tips and an iron-oxide surface. Figure 4 shows the effect of hydroxyl content on adhesion. As with the model hydroxylated surfaces, the individual bond strengths and hydrogen bond energies with the iron-oxide surface are consistent with hydrogen bonding interactions (Table II).

Decreasing the hydroxyl content on the cantilever tip did not have as significant an effect as on the model surface, as a 50% reduction in hydroxyl content was necessary to see a statistically significant decrease in the adhesion force. One reason for this is the uncertainty in the determination of the tip radius used to normalize the adhesion force. Another reason is that the iron-oxide surface is rough (for a $5 \times 5\ \mu m^2$ scan size, the RMS roughness ranged between 4 and 5 nm) and not fully hydroxylated but likely contains hydrophobic domains, decreasing the overall strength of interaction.

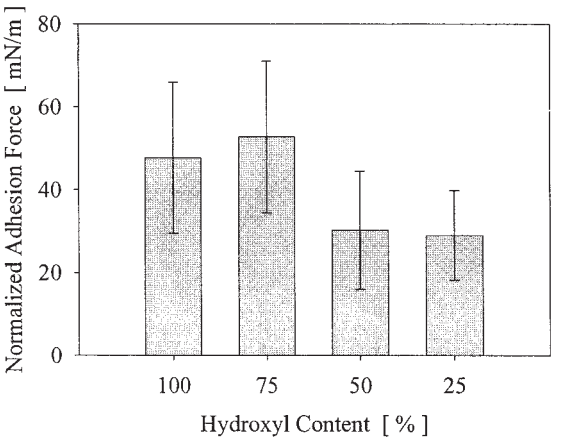

Figure 4 Average adhesion force (normalized by tip radius) between an iron-oxide surface and cantilever tips modified with different levels of hydroxy-functionalized alkanethiols.

The observed decrease in adhesion can be again explained in the framework of acid–base interactions in which the OH functionalized tip and the iron-oxide surface can act as a Brønsted acid and a base, respectively. With a decrease in the number of functional groups (OH) that can engage in acid–base interactions, the adhesion force decreases, accordingly.

Interaction between iron oxide and PVA: the effect of acetylation

A hydrophilic silica-glass sphere was chosen as a chemical mimic for cellulose —the main chemical constituent of paper—and the PVA adhesives were physisorbed onto the sphere surface by dip-coating (see Materials and Methods). Figure 5 shows that adhesion decreases with decreasing hydroxyl content (increasing degree of acetylation) of PVA. As was the case

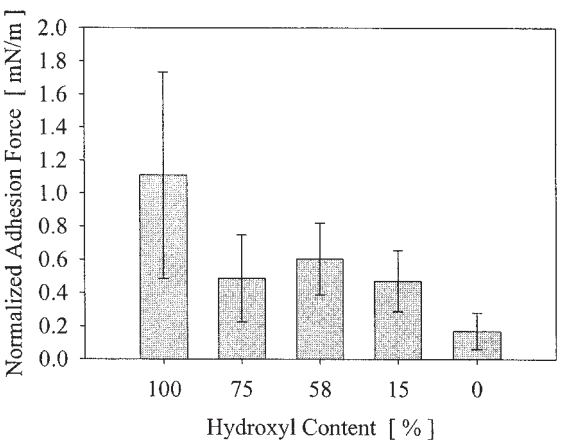

Figure 5 Average adhesion force between iron-oxide surface and colloidal probes modified with PVA with different hydroxyl content (degrees of acetylation).

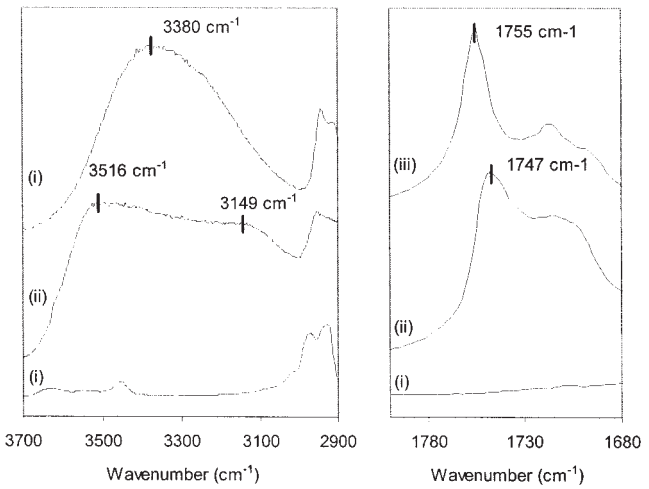

Figure 6 FTIR spectra of (i) PVA, (ii) PVAc25, and (iii) PVAc films in the (a) hydroxyl stretching (ν_{OH}) region and (b) carbonyl stretching (ν_{CO}) region.

with the hydroxyl-functionalized tip, this dependence can be understood in the framework of hydrogen bonding interactions.

Interestingly, a subtle increase in the degree of acetylation causes a significant drop in the adhesion force. This behavior may result from a significant conformational change in the polymer and a decrease in the effective number of hydroxyl groups able to interact with the iron-oxide surface. An increase in the degree of acetylation may likely cause a significant increase in intra/intermolecular hydrogen bonding because of the more polar (electronegative) nature of the carbonyl group, effectively tying up more hydroxyl groups. IR spectra support this argument in as much as the OH stretching region clearly splits into two, new broad bands, one shifted to lower and one shifted to higher wavenumber, indicating a significant change in hydrogen bonding [Fig. 6(a)]. The precise position of the hydroxyl group stretching frequency is an indication of the strength of hydrogen bonding present in the system.[28–31] The substantial increase in band intensity at the lower wavenumber region (3149 cm^{-1}) signifies the formation of strong hydrogen bonds. This band indicates a strong interaction involving the hydroxyl group and likely the carbonyl group (i.e., —O—H. . . O═C—).

Figure 6(b) shows the IR spectra in the carbonyl stretching region (1680–1800 cm^{-1}) of PVA (i), PVAc25 (ii), and PVAc (iii). As expected, the PVA does not have any stretching bands in this region, however, as with the hydroxyl stretching region [Fig. 6(a)], the incorporation of acetyl groups affects this region of the IR spectra. Compared to the fully acetylated PVAc (iii), the partially acetylated PVAc25 (ii) shows a different band center for this region, 1747 cm^{-1} versus 1755 cm^{-1}, respectively. The apparent wavenumber shift and broadening of this band is further evidence of the change in hydrogen bonding as a result of interaction between the carbonyl oxygen of the acetyl group and the hydroxyl group hydrogen.

The amount of acetylation also affected the shape of force–displacement curve. When retracting the colloidal probe from the iron-oxide surface, the initial unspecific adhesion peak is typically followed by molecular stretching events that finally subside at large surface separations. The frequency of occurrence of these stretching events decreased with increasing acetylation.

CONCLUSIONS

Atomic force microscopy was used to study the interactions between chemically modified surfaces to determine adhesion forces. Using modified AFM cantilevers and surfaces, the adhesion force between a hydroxyl-containing sample surface and a chemically functionalized tip was found to increase with increasing hydroxyl concentration on the probe tip. Individual bond forces and corresponding adhesive bond energies were derived from the sets of contact force data and found to be in the range of 10–40 kJ/mol; within the limits of hydrogen bond energies. Similar trends were observed with functionalized tips (SAM and polymer physisorbed colloidal probes) on a cast iron surface. Changing the degree of acetylation of the physisorbed PVAs changed the PVA conformation (and thus, the available hydroxyl groups for interaction with the iron-oxide surface) effectively decreasing the proton donating capability of the adhesive. The result was a significant effect on the adhesion force measurements on the iron-oxide surfaces consistent with acid–base interactions, more specifically hydrogen bonding, being the dominant adhesion mechanism in these systems. Therefore, these results suggest that adhesion forces in processes like paper creping can likely be controlled through tailoring "acid–base" interactions by carefully controlling of functionality of the applied adhesive.

References

1. van Ooij, W. J. In Physicochemical Aspects of Polymer Surfaces; Mittal, K. L., Ed.; Plenum: New York, 1983; p 1035.
2. Kinloch, A. J. Adhesion and Adhesives: Science and Technology; Chapman and Hall: London, 1987.
3. Israelachvili, J. Intermolecular and Surface Forces; Academic Press: San Diego, CA, 1992.
4. Wu, S. Polymer Interface and Adhesion, Marcel Dekker: New York, 1982.
5. Oliver, J. F. Tappi J 1980, 63, 91.
6. Chan, L. L. Presented at the Papermakers Conference: Proceedings of the Technical Association of the Pulp and Paper Industry, Portland, OR, April 25–27, 1983; p 197.

7. Sloan, J. H. Tappi J 1991, 74, 123.
8. Ampulski, R. S.; Sawdai, A. H.; Trokhan, P. D. Int. Pat. 9,302,252 (1993).
9. Vinson, K. D.; Weisman, P. T.; Phan, D. V. U.S. Pat. 5,487,813 (1996).
10. Oriaran, T. P.; Awofeso, A. O.; Kershaw, T. N.; Luu, P. V.; Neculescu, C. M.; Huss, M. E. U.S. Pat. 5,399,241 (1995).
11. Allen, A. J.; Sau, A. C. Eur. Pat. Appl. 814,108 (1997).
12. Janshoff, A.; Neitzert, M.; Oberdorfer, Y.; Fuchs, H. Angew Chem Int Ed Engl 2000, 39, 3212.
13. Noy, A.; Frisbie, C. D.; Rozsnyai, L. F.; Wrighton, M. S.; Lieber, C. M. J Am Chem Soc 1995, 117, 7943.
14. Binnig, G.; Quate, C. F.; Gerber, C. Phys Rev Lett 1986, 56, 930.
15. Florin, E. L.; Moy, V. T.; Gaub, H. E. Science 1994, 264, 415.
16. Binning, G.; Rohrer, H.; Gerber, C.; Weibel, E. Phys Rev Lett 1982, 49, 57.
17. Noy, A.; Vezenov, D. V.; Lieber, C. M. Annu Rev Mater Sci 1997, 27, 381.
18. Zauscher, S.; Klingenberg, D. J. J Colloid Interface Sci 2000, 229, 497.
19. Vezenov, D. V.; Noy, A.; Rozsnyai, L. F.; Lieber, C. M. J Am Chem Soc 1997, 119, 2006.
20. Sinniah, S. K.; Steel, A. B.; Miller, C. J; ReuttRobey, J. E. J Am Chem Soc 1996, 118, 8925.
21. Lee, G. U.; Chrisey, L. A.; Colton, R. J. Science 1994, 266, 771.
22. Ducker, W. A.; Senden, T. J.; Pashley, R. M. Nature 1991, 353, 239.
23. Ducker, W. A.; Senden, T. J.; Pashley, R. M. Langmuir 1992, 8, 1831.
24. Frisbie, C. D.; Rozsnyai, L. F.; Noy, A.; Wrighton, M. S.; Lieber, C. M. Science 1994, 265, 2071.
25. Koutsos, V.; Vegte, E. W. v. d.; Grim, P. C. M.; Hadziioannou, G. Macromolecules 1998, 31, 116.
26. Hutter, J. L.; Bechhoefer, J. Rev Sci Instrum 1993, 64, 1868.
27. Okabe, Y.; Akiba, U.; Fujihira, M. Appl Surf Sci 2000, 157, 398.
28. Drago, R. S.; Vogel, G. C. J Am Chem Soc 1992, 114, 9527.
29. Drago, R. S.; Obryan, N.; Vogel, G. C. J Am Chem Soc 1970, 92, 3924.
30. Joesten, M. D.; Drago, R. S. J Am Chem Soc 1962, 84, 3817.
31. Purcell, K. F.; Drago, R. S. J Am Chem Soc 1967, 89, 2874.